ALMA Memo 301

SSB vs. DSB for Submillimeter Receivers

James W. Lamb

Abstract— **A quasioptical image terminating diplexer may be placed before a double-sideband receiver to reduce the SSB system noise temperature. We present a detailed analysis that includes losses in the diplexer which indicates that the improvement is not as great as previously assumed. To achieve any worthwhile improvement the losses in the diplexer have to be kept very small (< 10 %) and the receiver noise temperature also has to be low. For a receiver DSB noise temperature of ~5*hν*/*k* the sensitivity improvement may be only ~10 % for moderate losses and atmospheric opacity. The same improvement can be achieved for a DSB receiver by reducing the noise temperature from 5*hν*/*k* to 4.2*hν*/*k*. A Dual-polarization DSB receiver is found to be a very competetive option**

I. Introduction

In an interferometric array the signal and image frequencies may be separated in the correlator, or the image may be removed by appropriate phase switching of pairs of local oscillators. The sole function of separating or dumping the image in the receiver is to remove some of the uncorrelated noise from the optics, antenna and atmosphere to improve the system sensitivity.

Various single-sideband (SSB) receiver configurations may be implemented. These may be divided into receivers based on image-rejecting mixers and receivers based on double-sideband mixers. In the image-rejecting mixer no noise is received through the image port, which is reactively terminated, but the receiver noise temperature may be higher than for the DSB mixer. We will not discuss this type of mixer further.

If double-sideband mixers are used input noise power in both sidebands will be converted to the IF. In the simplest configuration the upper and lower sidebands will both see the optics, antenna and atmospheric noise as well as the signal, but only the signal will be separated in the correlator. By adding an appropriate diplexer the image may be terminated in a cold load, which minimizes the noise for single-sideband observations. However only one sideband is now available for observing which may limit line-search and continuum observations. By adding another double-sideband (DSB) mixer to the other port of the diplexer (assuming it is a four-port type) the other sideband may be observed if there is sufficient correlator capacity.

Thompson and Kerr [1] and Jewell and Mangum [2] have considered some of the implications of these choices on overall system sensitivity. However the addition of a non-ideal diplexer to separate the two sidebands may also compromise the sensitivity in the signal band. This was not considered in the above memos, so this paper is intended to quantify the effects of an imperfect diplexer on system sensitivity.

11 April, 2000

Owens Valley Radio Observatory, California Institute of Technology, Big Pine, CA 93513, USA

II. The Receiver model

Fig. 1 shows a signal flow diagram of the receiver to define the terms used in the calculations of system temperature. The device used to separate the upper and lower sidebands has four physical ports: **S** for the signal input from the antenna, **I**, the image load termination port, **U**, the output port for the upper sideband, and **L**, the output port for the lower sideband. Each of these physical ports can be regarded as two signal ports, one at the upper sideband frequency and the other at the lower, as shown on the diagram, giving a total of eight ports.

Port **S** is connected to the antenna and has an input power spectral density represented by the Rayleigh-Jeans (RJ) equivalent noise temperature T_{ant}. As discussed below this includes all noise sources in front of the receiver including atmosphere, antenna, etc. The image port **I** is connected to an image dumping load which we suppose to be perfectly matched and at a physical temperature $\boldsymbol{T}_d$ (physical temperatures will be denoted using boldface and RJ equivalent temperatures by regular face type).

In an ***image dumping*** receiver a DSB mixer is connected to one of the ports, which we assume here to be the USB port. By adding a second DSB mixer to the other port we obtain an ***image-separating*** receiver.

Assuming that all the ports are well matched there are eight relevant transmission coefficients as shown in Fig. 1. Each efficiency η has a subscript denoting the physical ports and a superscript indicating the frequency sideband. For example, $\eta_{U,I}^{USB}$ is the fraction of the noise in the upper sideband frequency band generated by the image dump that is transmitted to the **U**-port. Nominally this should be zero since this port is intended to transmit the USB from the antenna but not from the image load. All the coefficients are independent within the constraints of power conservation. To make the problem more tractable we will analyze only the USB mixer and assume that

$$\begin{aligned} \eta_1 &= \eta_{U,S}^{USB} = \eta_{U,I}^{LSB} \le 1 \\ \eta_2 &= \eta_{U,I}^{USB} = \eta_{U,S}^{LSB} << 1 \end{aligned} \tag{1}$$

A similar set would apply to the lower mixer if present. These coefficients can be combined to give an image rejection ratio

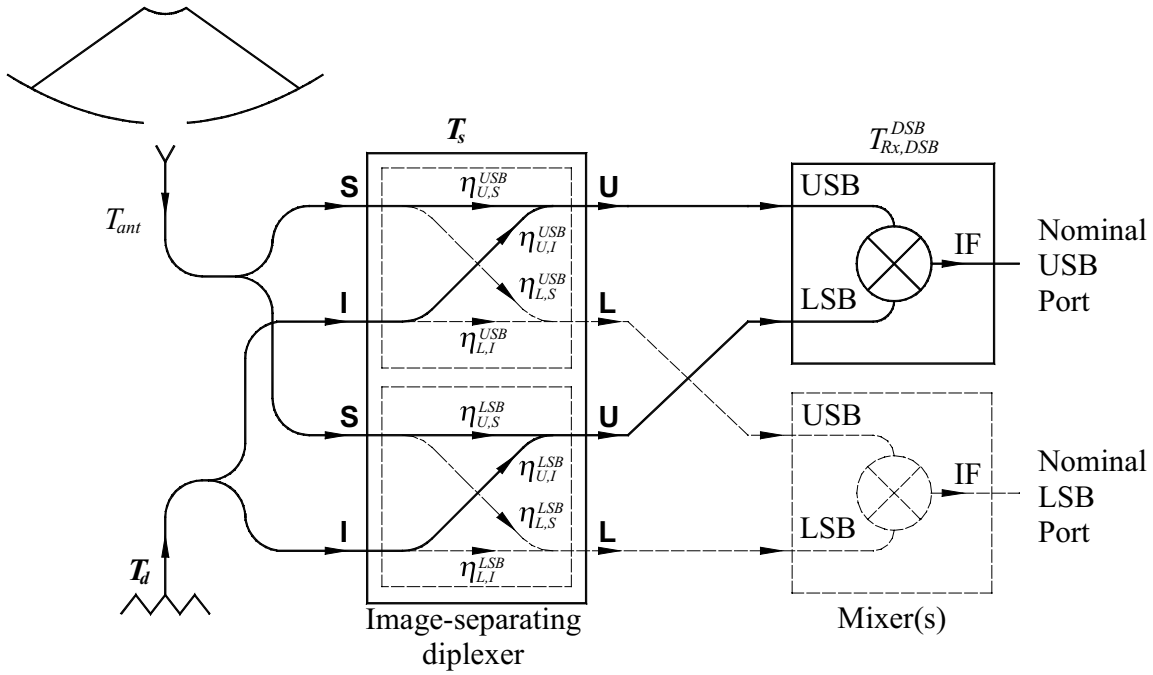

Fig. 1. Signal flow diagram for receiver with image separating diplexer at a physical temperature T_s. The temperature of the dump on the image port is T_d. **S** is the physical port where the sky signal enters the diplexer and **I** is the port where the noise from the image termination enters. **U** is the port from which the upper sideband is extracted while the the lower sideband is taken from port **L**. In an image dumping receiver only the upper mixer is present. Adding the lower mixer (broken line) allows both sidebands to be measured simultaneously. It is assumed that the mixer has equal gain in the two sidebands.

$$R = \eta_1 / \eta_2 \tag{2}$$

and a loss in the diplexer

$$L = (\eta_1 + \eta_2)^{-1} \tag{3}$$

The rejection ratio and loss will depend on the type of diplexer, bandwidth, component non-ideallity, overlap loss, etc. It is important to recognize that (1) implies that the USB and LSB responses are complementary and that the following should not be applied to a DSB tuning of the diplexer (white light fringe).

In the previous memos the reduction in signal due to η_1 and the added noise due to L were not considered.

III. NOISE TEMPERATURES

Since the effects on system sensitivity will be presented as relative improvements or degradations the choice of reference plane where the system noise temperature is calculated is not important. For the analysis the reference plane for the system temperature will be taken as the input to the receiver, with the diplexer being included as part of the receiver.

Following the earlier memos [1], [2] we will write the RJ equivalent temperature T of a physical temperature $\boldsymbol{T}$ at some frequency, ν, as

$$T(\nu, \boldsymbol{T}) = \frac{\frac{h\nu}{k}}{\exp\left(\frac{h\nu}{k\boldsymbol{T}}\right) - 1} \tag{4}$$

Fig. 2 shows the ratio of the radiation temperature to the physical temperature over the frequency range of the array for various temperatures. In the sub-millimeter there are significant reductions in noise power for blackbodies with physical temperatures of $\boldsymbol{T} < 30$ K.

Antenna noise comprises several components. Source signal noise is ignored here, but we include the cosmic background radiation with a physical temperature $\boldsymbol{T}_{bg}$

$$\boldsymbol{T}_{bg} = 2.7 \text{ K} \tag{5}$$

Atmospheric emission depends on the zenith opacity, τ_0, the number of air masses, A, and the temperature of the atmosphere, $\boldsymbol{T}_{atm}$. To estimate the atmospheric temperature we take, following Jewell and Mangum [2]

$$\boldsymbol{T}_{atm} = 0.95\ \boldsymbol{T}_{amb} \tag{6}$$

where $\boldsymbol{T}_{amb}$ is the ambient temperature at ground level. If the ambient spillover efficiency (including ohmic losses, etc.) of the antenna is η_{sp}, then the effective antenna noise temperature at the receiver plane will be

$$T_{ant}(\nu) = \eta_{sp} T_{atm}(1 - \exp(-A\tau_0)) + (1 - \eta_{sp}) T_{amb} + \eta_{sp} T_{bg} \exp(-A\tau_0) \tag{7}$$

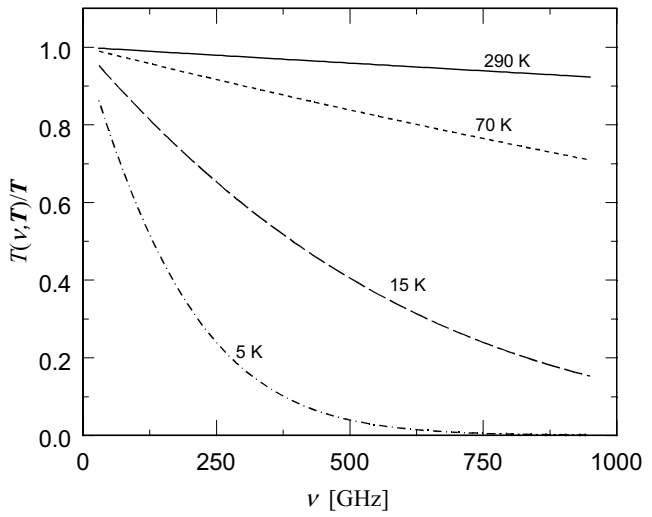

Fig. 2. Reduction of effective radiation temperature relative to physical temperature for various blackbody temperatures.

Note that this uses the effective radiation temperatures rather than the physical ones.

If $T_{Rx,DSB}^{DSB}$ is the DSB receiver noise temperature then the SSB temperature of the system in the absence of the signal/image separating optics is

$$T_{sys,SSB}^{DSB} = 2\left(T_{Rx}^{DSB} + T_{ant}\right) \tag{8}$$

while the SSB temperature with the separating optics is

$$T_{sys,SSB}^{SSB} = \left(1+\frac{1}{R}\right)\left(2LT_{Rx,DSB}^{DSB} + 2(L-1)T_s + T_d + T_{ant}\right) \tag{9}$$

The superscript indicates whether the system is nominally single- or double-sideband. With infinite rejection loss and no internal losses this gives

$$T_{sys,SSB}^{SSB} = 2T_{Rx,DSB}^{DSB} + T_d + T_{ant}, \quad R \to \infty, L = 1 \tag{10}$$

as expected.

A factor which quantifies the improvement resulting from the addition of the diplexer, Γ, can be defined by

$$= \frac{T_{sys,SSB}^{DSB}}{T_{sys,SSB}^{SSB}} \tag{11}$$

This takes into account almost all factors affecting sensitivity apart from some minor factors, such as optics aberrations, which affect the aperture efficiency.

For a perfect diplexer ($R \to \infty$, $L = 1$) Γ will be greater than one, provided the effective radiation temperature of the image load is less than the antenna noise temperature (which will be dominated by sky noise). Clearly the image load has to be cryogenically cooled.

IV. Examples

Two examples are given: a 650 GHz receiver and a 950 GHz receiver. The parameters used are shown in Table I. Where several values are given results are presented for each of the values. The opacities correspond to the first quartile calculated from the 220 GHz tipper data [3] with conversion factors derived from measured data [4]. The number of air masses, 1.3, corresponds to a source elevation of 50°.

TABLE I
PARAMETER VALUES USED IN CALCULATIONS.

Parameter	Symbol	Value
Cosmic background	T_{bg}	2.7 K
Ambient temperature	T_{amb}	270 K
Atmosphere temperature	T_{atm}	257 K
Antenna spillover efficiency	η_{sp}	96 %
Zenith opacity		
650 GHz	τ_0	0.8
950 GHz	τ_0	1.5
Air masses (El = 50°)	A	1.3
Separating optics temperature	T_s	290 K
		70 K
		15 K
		5 K
Image dump temperature	T_d	290 K
		70 K
		15 K
		5 K
Receiver DSB noise temperature	$T_{Rx,DSB}^{DSB}$	$2h\nu/k$ — $5h\nu/k$
Rejection ratio	R	∞
		10 dB
Loss	L	0 dB
		0.45 dB (10 %)

Fig. 3 and Fig. 4 show the sensitivity improvement resulting from image rejection as a function of receiver noise temperature. The thick lines with filled symbols show the effect of image termination on a system with a perfect image diplexer. For both frequency bands there is a significant improvement with cooling the image load from 70 K to 15 K, but only a small gain going from 15 K to 5 K.

The thin line with filled symbols represents a system with a diplexer having no ohmic losses, but imperfect image rejection of 10 dB (due, for example, to overlap losses or the integrated effect over a sinusoidal passband). Although all the noise power comes either from the antenna or the image load there is still a significant reduction in sensitivity compared to the perfect case.

The thin lines with the open symbols correspond to a diplexer with imperfect image rejection and some additional losses at the temperature of the diplexer. Having the image load cooled but the diplexer at ambient temperature gives no reduction in system noise unless the intrinsic receiver noise is also low. Even with a very low receiver noise temperature the

improvement is only ~10–15 %. Cooling the optics is clearly necessary, even if it requires having mechanisms operating at cryogenic temperatures. If the optics are cooled they should preferably be at ~20 K or below.

Comparing the overall estimates for the 650 GHz and the 950 GHz receivers there is less improvement for the higher band. Although the assumed atmospheric transparency is lower there, the receiver noise temperature is higher and

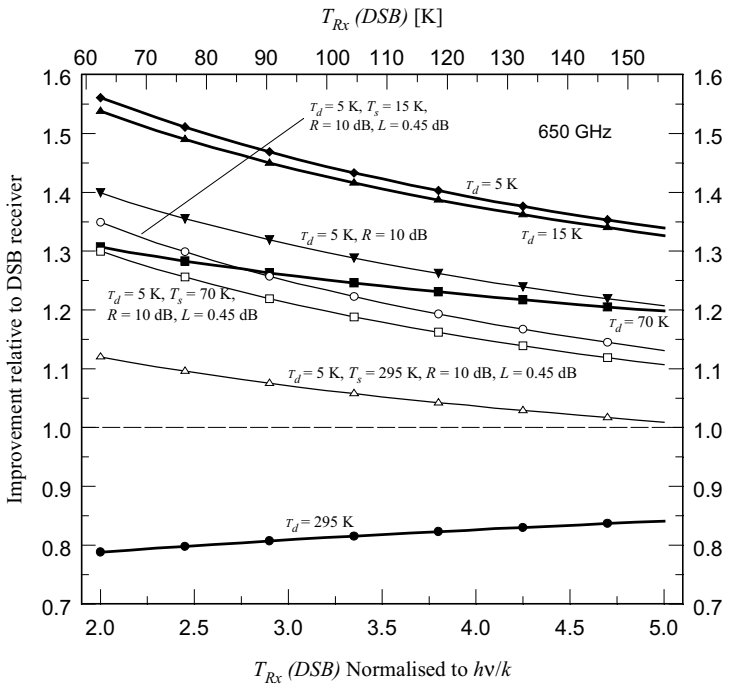

Fig. 3. Graph showing the improvement of a 650 GHz system noise temperature as a function of receiver noise temperature for various image dumping diplexer parameters. Unless otherwise noted $R \rightarrow \infty$ and $L = 1$. For non-lossy diplexers the temperature of the diplexer itself does not affect the results. See text and Table I for assumptions about atmospheric opacity, etc.

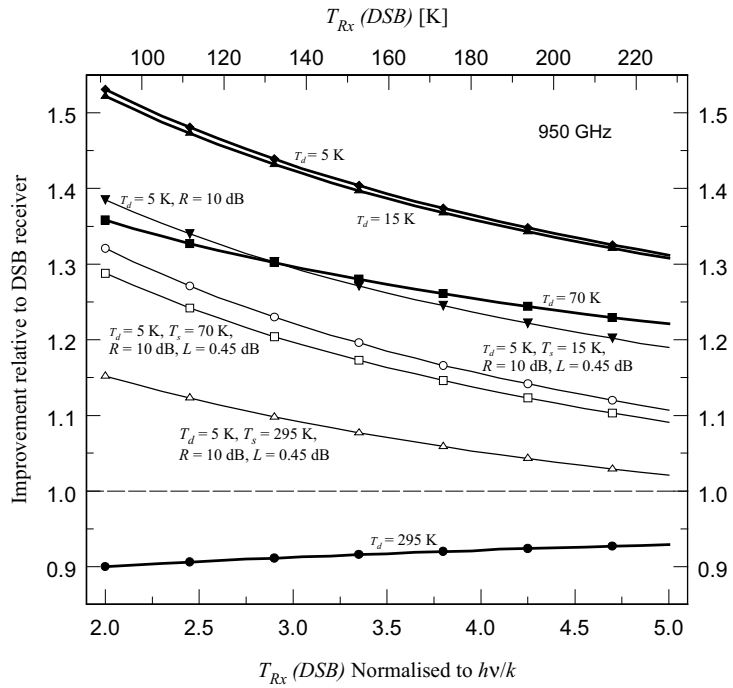

Fig. 4. Graph showing the improvement of a 950 GHz system noise temperature as a function of receiver noise temperature for various image dumping diplexer parameters.

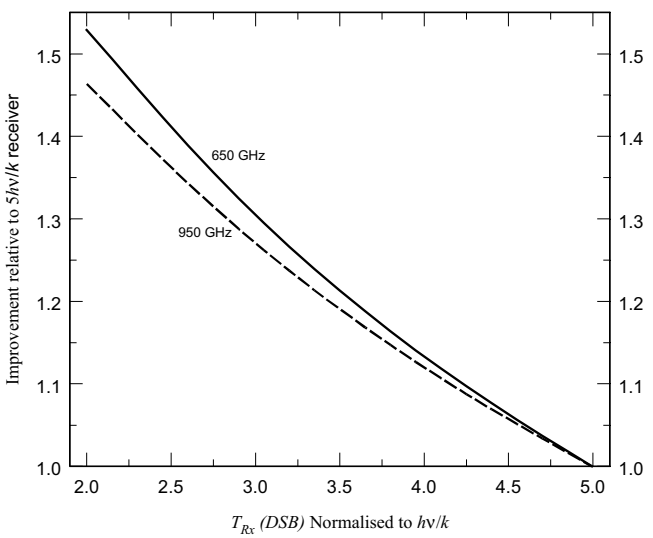

Fig. 5. Improvement in sensitivity resulting from reduction in intrinsic receiver noise. Antenna and atmosphere parameters are as in Table I.

therefore a larger fraction of the total noise contribution.

Currently receiver temperatures are closer to $5h\nu/k$ than $2h\nu/k$, so the improvements afforded by image dumping or separation are not as significant as they could be. For comparison, Fig. 5 shows the increase in system sensitivity that could be achieved by reducing receiver noise.

V. Discussion

When realistic assumptions are made about how image separation is done in a sub-millimeter receiver the advantage in terms of sensitivity is greatly reduced compared to the ideal case. To achieve significant improvements both the rejection ratio and the losses in the diplexer must be kept low, which may be difficult at sub-mm wavelengths. Measurements of the loss of the Martin-Puplett diplexer used on the 1-mm receiver at the NRAO 12-m telescope gave a value of 7–10 %, so that the value of 10 % used here may even be pessimistic considering the factor of four or so in frequency. The values of 10 dB for the average rejection across the IF band is realistic for the wide bandwidths to be used. These two contributions can reduce the expected advantage of the image-dumping system from ~30 % to ~10 % in sensitivity for current receiver noise temperatures.

Curves in Fig. 3 and Fig. 4 are given for the first quartile opacities and it is unlikely that observations would be made under worse conditions since the opacity would still be excellent at millimeter wavelengths. The better part of the quartile may be used for observations near the edges of the band, so the values used in the computations should be representative of a large fraction of the observing conditions.

For sources above 30° elevation the average number of airmasses is 1.1 [5] so that the value of 1.3 used here is conservative.

Simultaneous measurements of spectral lines separated by more than the IF bandwidth and continuum observations can both benefit from a DSB system. If an SSB receiver is to be competitive it needs to result in an SSB system temperature, $T_{sys,SSB}^{SSB}$, which is √2 lower than the SSB temperature of the DSB system, $T_{sys,SSB}^{DSB}$, so that the total integration time is the same [1]. For the parameters values assumed here this would not be the case. In principle the image diplexer could be set to zero path difference to match the system to the observations, but there would still be some degradation compared to a receiver with no diplexer. If an image-separating receiver is used the DSB and SSB versions would be almost equivalent, but the correlator bandwidth requirement is doubled.

In addition to the sensitivity trade-offs the complexity of the system has to be considered. Addition of a quasioptical diplexer with moving elements will increase the size of the dewar, reduce reliability and increase development and construction time and budgets. Table II shows the choices of possible receiver configurations ranked in order of complexity. The sensitivity ranking is relative and does not indicate how large the differences are. Depending on the conditions and the optical losses the improvement in sensitivity for an image-dumping receiver will be in the range of 5–15 % for single-sideband observations. For double-sideband observations there will be a loss of 25–35 %. Even for low noise receivers the improvement factor does not exceed 1.4 for reasonable parameters. This means, for example, that it is always better to use two mixers in a dual polarization system than to use them in an image-separating mixer if a single grid can be used for the polarization diplexer. The sensitivity ranking in Table II is therefore independent of the basic receiver noise.

TABLE II
RECEIVER CONFIGURATIONS IN ASCENDING COMPLEXITY. THE "SENS." COLUMNS RANK THE SENSITIVITY FOR THE GIVEN OBSERVING MODES. "POL." IS THE NUMBER OF POLARIZATIONS.

	Description	# Mixers	# Pol.	Sens. SSB	Sens. DSB
1	One DSB receiver	1	1	5	3
2	Two DSB receivers	2	2	3	2
3	One image dumping receiver[1]	1	1	4	6
4	One image separating receiver[1]	2	1	4	4[2]
5	Two image dumping receivers[1]	2	2	2	5[2]
6	Two image separating receivers[1]	4	2	1	1

Notes: [1] See Section II for definitions. [2] These are almost the same, but 5 requires the addition of a polarizing grid.

One question that remains open is how the sidebands will be separated or removed in single dish observing. This is primarily an issue of line confusion since the sideband ratio calibration may be done interferometrically. Possible options are to have special receivers for those antennas which will be used in single-dish mode, or to separate or smear the

sidebands by moving the LO as has been done at the CSO and NRAO 12-m observatories. This requirement has implications for the frequency resolution of the first local oscillator reference.

VI. Conclusions

It is difficult to be categorical in deciding whether or not to implement a sideband-separating scheme but it is clear that there are significant technical hurdles to overcome to achieving modest improvements in sensitivity. In the long term it is likely that image separating mixers will be developed in a compact (waveguide or planar integrated) form. If the science mix includes a significant fraction of DSB observations then Table II shows that a simple dual polarization DSB receiver is very competetive and may be exceeded only by a full four-mixer design.

Looking for a reasonable implementation path we would suggest that dual-polarization receivers with DSB mixers should be the first step. Design and construction of 140 such mixers is already an enormous task. In parallel, development of more sophisticated image separating/balanced mixers can proceed. SIS mixers were first used on telescopes over 20 years ago but there is still no integrated sideband separating mixer being used for observations.

References

[1] A. R. Thompson and A. R. Kerr: “Relative sensitivities of single and double sideband receivers for the MMA,” ALMA Memo No. 168, April 1997.

[2] P. R. Jewell and J. G. Mangum: “System temperatures, single versus double sideband operation, and optimum receiver performance,” ALMA Memo No. 170, May 1997.

[3] NRAO ALMA Web Site: http://www.tuc.nrao.edu/mma/sites/Chajnantor/data.c.html, as of 5 April, 2000.

[4] S. Matsushita, H. Matsuo, J. R. Pardo, and S. J. E. Radford: “FTS measurements of submillimeter-wave atmospheric opacity at Pampa la Bola II: supra-terahertz windows and model fitting,” *PASJ*, vol. 51, p. 603, 1999.

[5] S. J. E. Radford, Private communication.